



The Society shall not be responsible for statements or opinions advanced in papers or discussion at meetings of the Society or of its Divisions or Sections, or printed in its publications. Discussion is printed only if the paper is published in an ASME Journal. Authorization to photocopy for internal or personal use is granted to libraries and other users registered with the Copyright Clearance Center (CCC) provided \$3/article is paid to CCC, 222 Rosewood Dr., Danvers, MA 01923. Requests for special permission or bulk reproduction should be addressed to the ASME Technical Publishing Department.

Copyright © 1999 by ASME

All Rights Reserved

Printed in U.S.A.

**ON THE DEVELOPMENT AND APPLICATION OF THE FRAP® (FAST-RESPONSE AERODYNAMIC PROBE) SYSTEM IN TURBOMACHINES - PART 3: COMPARISON OF AVERAGING METHODS APPLIED TO CENTRIFUGAL COMPRESSOR MEASUREMENTS**

Pascal Köppel, Christian Roduner, Peter Kupferschmied, Georg Gyarmathy



Turbomachinery Laboratory  
Institute of Energy Technology  
**ETH** - Swiss Federal Institute of Technology  
8092 Zurich, Switzerland  
<http://www.lsm.iet.ethz.ch/lsm/>

**ABSTRACT**

Typically several hundred million data points arise from a comprehensive measurement campaign carried out in a centrifugal compressor test rig with the FRAP® system (see Part 1). In order to obtain a maximum of information about the unsteady flow at any position in this turbo machine the time-resolved data processing method has to be optimized. In contrast to the standard time-averaged flow measurements with pneumatic probes, the objective of FRAP® measurements and of data processing is to extract novel information about crucial unsteady phenomena like turbulence, row-to-row interaction, modal or rotating stall, leakage flow effects etc. In such cases the simultaneous measurement of static and total pressures and flow vectors is of particular interest. Novel information means the analysis of averaged and time-resolved (wavelet) spectra, autocorrelations or time averages properly conserving physical fluxes, etc..

Different averaging methods are applied to compress the time dependent data measured by a I-sensor-probe (see Part 2) in a centrifugal compressor. Such results could be used for comparison with pneumatic sensor measurements and CFD calculations. The comparison of averaging methods includes the averaging theories by TRAUPEL and by DZUNG which are compared to simple arithmetic time averaging. From there the specific stage work is calculated.

In analysing the time dependency several ensemble-averaging procedures for flow pressure and velocity are utilized for separating deterministic from stochastic fluctuations, extracting blade row finger prints or investigating low-frequency surge type fluctuations.

With respect to the selection and overall optimization of data processing methods an overview of generic tools is given and the modularity of the processing procedures is discussed.

**NOMENCLATURE**

A area

$\Delta A$	area for the mass flow calculation
a	confidential interval
$a_a$	specific stage work
b	diffuser width (axial)
C	specific speed
$C(P,m)$	coefficient of Gauss distribution
c	velocity
$c_p$	specific heat at constant pressure
f	frequency
$f_A$	sampling frequency
h	enthalpy
i	summation index
L	length of diffuser vane
M	Mach number
m	Number of shaft revolutions or blade twin passing
$Mu$	impeller tip speed Mach number
$\dot{m}$	mass flow
n	number of measured data
N	number of shaft revolution per seconds
p	pressure
R	gas constant
r	radius, recovery factor
$r^*$	Euler radius
s	specific entropy
T	temperature
$T_{rec}$	recovery temperature
t	time
$t_R$	time of one impeller revolution
$t_T$	time of a twin blade passing
$t_0$	total measurement time
u	circumferential speed
$\dot{V}$	flow rate
X	flow quantity
z	axial coordinate

$\alpha$	flow angle (diffuser coordinates)
$\alpha_{B \text{ vane}}$	diffuser vane leading edge blade angle
$\eta^\circ$	isentropic efficiency (total-to-total)
$\theta$	azimuth angle
$\rho$	density
$\epsilon_k, \epsilon_c$	shape factors of Traupel
$\sigma$	standard deviation
$\varphi$	yaw flow angle (probe coordinates)
$v$	specific volume
$\varphi$	flow coefficient $\left( \varphi = \frac{\dot{V}_1}{D_2^2 \cdot u_2} \right)$
$\omega$	impeller angular velocity
<b>Superscripts</b>	
-	averaged over time, or z, or time and z, Eq. (6) to Eq. (8)
~	ensemble averaged over time
<b>Subscripts</b>	
1,2,3	sensor yaw positions
1	impeller inlet
2	impeller outlet, ( $r_2=140\text{mm}$ )
Dz	averaged with the method of Dzung
E	measurement position $r_E=147\text{mm}$
i	summation index
n	ensemble-averaged time index
r	radial direction
stat	static flow properties
t	tangential direction
tot	total flow properties
z	axial direction

## INTRODUCTION

A measurement campaign using the fast-response aerodynamic probe technology of the ETH (FRAP<sup>®</sup>) was performed in a single stage centrifugal compressor running at two operating points, „best point“ (BP) and „mild surge“ (MS) conditions. The complex and highly fluctuating flow field found close to the outlet of centrifugal impellers (e.g. TRAUPEL 1988, DEAN and SENOO 1960, ECKARDT 1975) is suitable for demonstrating the capabilities of the FRAP<sup>®</sup> System, for testing measurement concepts and data processing methods, and for confronting different averaging methods.

The huge amount of time-resolved data requires an optimization of data processing methods including the optimization of measurement objectives, measurement concepts and of the data evaluation software and of the data analysis and interpretation procedures. For measurements during MS running conditions, a special triggering and traversing concept and a different ensemble definition had to be established.

Data averaging is one of the key topics in data processing (e.g. ADAMCZYK 1985, GERHARD 1981, KREITMEIER 1997). In the first part of this contribution, the ensemble averaging methods, including circumferential, blade to blade ensemble (e.g. Ng 1985, Ruck 1989) and flow-based averaging methods (see Part 2) will be compared. Using these, information about deterministic (related, for example to rotor position) and stochastic (related, for example, to turbulence) fluctuations can be gained and the harmonic time-dependent characteristics of the data can be preserved. In the second part, the oversimplified arithmetic averaging is compared with the physically founded

averaging methods of TRAUPEL (1988) and DZUNG (1967, 1970). In these methods, the averages of physical conserved flow quantities comply with the conservation equations such as momentum balance, mass balance, moment of momentum balance or energy balance.

Additionally, the influence of different averaging methods on the value of the stage work is presented.

## TEST RIG, INSTRUMENTATION AND MEASUREMENT SYSTEM

The closed loop test rig where the experiments were carried out is described in more detail in Part 2 of this contribution and in RODNER et al. (1998). The centrifugal compressor Fig. 1 is a standard industrial stage. The present measurements were made at a shaft speed of 17720 rpm at two running conditions given in Table 1. The main data of the impeller were:

impeller tip diameter ( $2r_2$ )	280 mm
full/splitter blades	11/11 (total 22)
exit blade angle	30° back lean
exit width b	16.8 mm
diffuser vanes	24
diffuser vane inlet angle	25° from tangential

Every second impeller blade being different („full“ vs. „splitter“, see Fig. 1), every second impeller channel will have a noticeably different exit flow. The radial diffuser has parallel plane walls and is followed by a large toroidal collecting chamber (not shown) providing a virtually uniform circumferential pressure distribution at the diffuser outlet (HUNZIKER 1993).

### Measurement System

**Aerodynamic probes.** The measurements treated herein were carried out by our fast response aerodynamic probes termed FRAP<sup>®</sup>. More details about the FRAP<sup>®</sup> System are given in Part 1 of this contribution and in GOSSWEILER et. al. (1992,1995).

The straight cylindrical FRAP<sup>®</sup> 1-sensor probes used here (Fig.1) have a tip diameter of 1.8mm with one piezoresistive pressure sensor chips inside the probe. The useful temperature limit of the sensor is about 140°C. The uncertainty of the pressure measurement is typically 0.2 mbar (standard deviation) after adjustment; i.e. about 0.09% of the dynamic head in the present case. The sampling frequency of the signals is 200kHz maximum and the useful frequency bandwidth is 44kHz after signal filtering with an analog anti-aliasing filter, in contrast to the 6.5kHz blade passing frequency. The sensor calibration, the aerodynamic probe calibration and the operating concepts are described in more detail in Part 1 and KUPFERSCHMIED (1994, 1998).

**Probe control and data acquisition.** To be able to measure with the FRAP<sup>®</sup> system in special flow conditions (e.g. during MS in the compressor system) complex measurement procedures are necessary. These procedures must comply with the objectives and requirements of the data analysis and are called *measurement concepts* in the following. To achieve high accuracy and good repeatability a high automatization of the operating system is required. The probe control unit, the reference pressure control unit and all auxiliaries are computer controlled.

## EXPERIMENTAL SET-UP AND MEASUREMENT PROCEDURE

The probe was mounted at Position I near the exit of the impeller,

Fig. 2. for the present measurements. Flow traverses are made by moving the probe in axial direction with the sensor tap moving from the rear to the front wall in 13 positions. Fig. 1. Only 5 traverse points were taken for the measurements during MS.

As described in STAHLCKER and GYARMATHY (1998), high circumferential and radial velocity components exist at position I and the axial component is low (nearly planar flow). This justifies the use of a 1-sensor fast-response probe in a pseudo-3-sensor mode (see Part 1 and Part 2) to provide the 2D velocity components only.

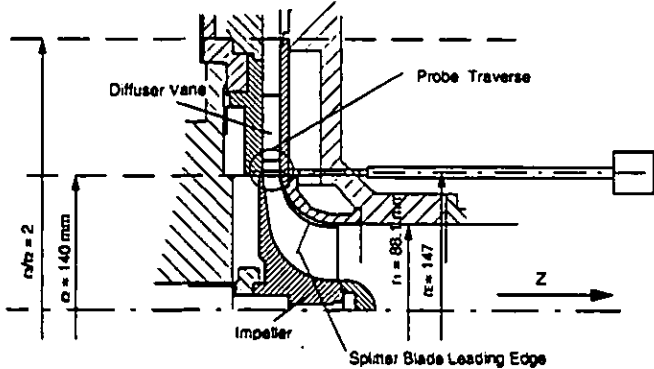


Fig. 1 Cross-sectional view of the centrifugal compressor with FRAP<sup>®</sup> probe

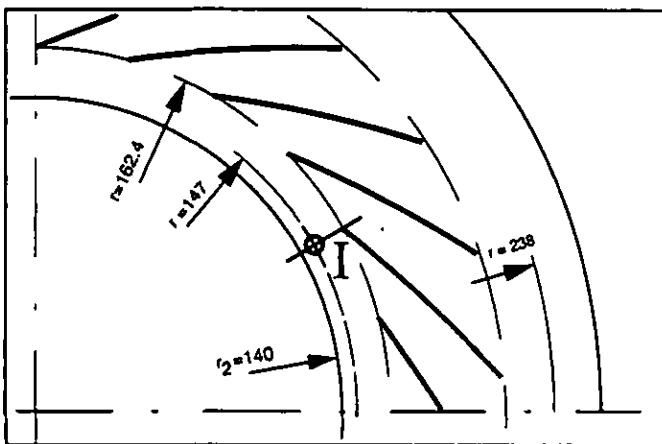


Fig. 2 Top view of the diffuser showing probe position I

	„best point“ (BP)	„mild surge“ (MS)
RPM	17720	17720
$\dot{V}$ [m <sup>3</sup> /s]	1.553	1.052
$\dot{m}$ [kg/s]	1.757	1.192
$\phi$ [-]	0.0768	0.0521

Table 1 Operating points of the centrifugal compressor for the measurements presented

### DATA PROCESSING - CONVERSION AND ANALYSIS OF TIME-RESOLVED DATA

#### FRAP<sup>®</sup> data processing.

In this measurement campaign more than 280 million data points were collected. The processing of these has to consider several requirements such as the handling by suitable software programs, the conversion of the signals from voltage to flow quantities and the appropriate presentation of the results. To compare the time-resolved flow quantities, such as velocity or flow angle, with time-mean data measured with pneumatic probes, data averaging methods are useful to compress the data mound. Fig. 3 shows the time-average flow angle variation across the flow channel in the foreground. To obtain the time averaged data point at any one traverse position, nearly a million pressure values were measured, converted into flow angle values and suitably averaged to give the black dots shown. A short part of the time resolved value chains (about 0.5%) are indicated for two of the dots.

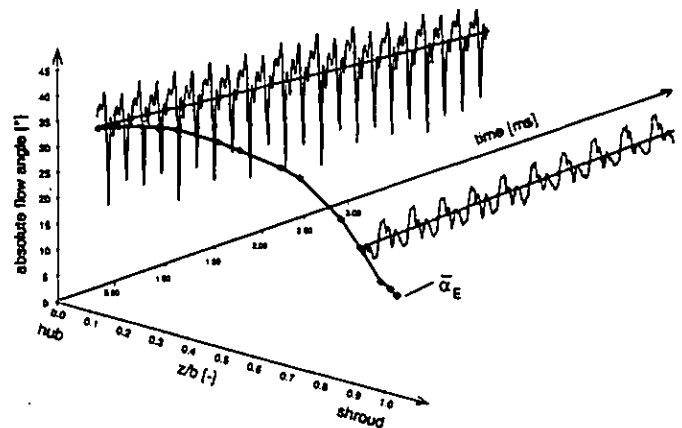


Fig. 3 Example: Compression of the time-resolved absolute flow angle  $\alpha_E$  into the time-averaged distribution of  $\bar{\alpha}_E$  over the traverse

#### Conceptual questions

The example in Fig. 3 shows the amount of information contained

in the measured FRAP<sup>®</sup> data. A lot of questions arise in connection with such large amounts of data. Some questions are more of generic nature:

- What information can be gained from the measured data?
- How to get a maximum of information?
- What can FRAP<sup>®</sup> data be used for?

More specific questions are

- Which flow quantities can be obtained and what are the uncertainties?
- How should the flow quantities be averaged?
- Which quantities of turbulence are measurable?
- Are there unsteady physical phenomena that cannot be detected?

Questions with respect to the organizational procedures are

- How should a measurement campaign be planned and performed for specific objectives?
- What are the experiences from FRAP<sup>®</sup> measurement campaigns?
- How can the costs of a measurement campaign be optimized with appropriate measurement concepts?

### Objectives of the measurement campaign

The objectives will determine measurement concepts, the data to be obtained and their refined evaluation. In the present measurement campaign in the centrifugal compressor two classes of objectives have been set, one concerning the measurement system and the other the physical flow situation in the machine. Class 1 objectives were:

- To test the in-house developed fast-response aerodynamic probe technology (FRAP<sup>®</sup>) in a high speed turbomachine.
- To compare different averaging methods for the stage work, the static pressure and the radial velocity obtained at the impeller outlet.
- To explore flow phenomena such as „mild surge“ and rotating stall by means of special measurement concepts and averaging methods. (Only MS data are discussed in Part 3.)

Class 2 objectives were:

- To make detailed time-resolved measurement at the impeller outlet and at different points in a vaned diffuser channel.
- To provide experimental boundary conditions for CFD calculations in the vaned diffuser (CASARTELLI et al. 1997).

### Measurement concepts used.

The measurement concept must define the probe type, and the traverses to be made. It must take into account the key data of the machine, hence determine the characteristic data of the measurement campaign.

**Probe type and probe operation mode.** For the objectives defined above a 1-sensor fast-response probe used in a pseudo-3-sensor mode has been chosen. At every traverse position the fluctuating flow was measured time-resolved under three angular positions of the probe shaft. The middle of the three angle positions was set to the time-averaged flow direction at the local axial position. For the other two angle positions the probe was rotated (in yaw) by  $\pm 43^\circ$ . A once per revolution signal from the trigger was used to fit the sensor signals together to a quasi-synchronous pseudo-3-sensor probe (Part 1).

**Traversing.** According to the objectives of the measurement campaign it is necessary to get the time dependent information over the height of the diffuser channel in axial direction. To resolve gradients in the diffuser channel, the traverse points have to be close to each other. Per traverse 13 traverse points were taken at each yaw position. The measurements presented in this paper were taken at position I (Fig. 2).

**Key compressor data and planning the measurement campaign.** In Table 2 the parameter choices associated to the objectives of the measurement campaign and the key data of the compressor are shown.

In the first part of Table 2 the dominant frequencies of the compressor and the resulting setting ranges for the measurement system are listed. In the middle part on the left side the maximum peaks of the compressor flow quantities are listed. On the right side the resulting resolution of the sensor signals and the calibration ranges are determined. In the bottom part the spatial resolution by the probe and the expected spatial dimension of turbulence are listed.

Key data of the machine		Characteristic data of the measurement campaign	
Impeller RPM	17720rpm	Number of points per traverses for BP	13
Number of Blades $z_b$	22	Number of data points between 2 blades	31
Blade passing frequency: $f_{bp} = 2 f_{z_b}$	$f_{bp} = 6.5\text{kHz}$	Sampling frequency $f_s$ for „best point“	200 kHz
Other important frequencies	$f_{blade\ surge} = 18\text{Hz}$ $f_{rotational\ stall} = 42\text{Hz}$	Data length (measuring time)	163840 points (0.82s)
		Number of revolutions per averaging	242
		95% confidential interval for ensemble averaging	$a = 7.9\text{mbar}$ $a/\sigma = 7.9/63 = 0.1$
Dynamic head	$\approx 220\text{mbar}$	Accuracy of the sensor (signal/noise ratio)	$220/0.07 = 3142$ 70dB
		Sensor sensitivity	6.3mV/mbar
Max. pressure peak	2200mbar	Reference pressure in the probe shaft (absolute)	1700mbar
Averaged pressure	1510mbar		
Max. pressure fluctuation	Max: 814mbar (peak to peak)	Range of the voltage signals from sensor	$\pm 5\text{ V}$ for U $\pm 10\text{ V}$ for Ue
		Resolution of the sensor pressure signals for $\pm 5\text{V}$	0.4 mbar (12 bit)
Max. angle fluctuation	$\Delta\varphi = 16.6^\circ$	Calibration range of the yaw angle	$\varphi = \pm 20^\circ$
Mach number	0.75	Calibration range of the Mach number	$0.2 < M < 0.7$
Max. temperature	63.1°C	Number of offset and gain adjustments	2 per traverse
		Spatial resolution of the probe ( $d_{probe}$ )	$d_{probe} = 1.2\text{mm}$
Spatial dimension of a fluid part ( $f_{turbulence} = 44\text{kHz}$ )	$d_{probe} = 4.4\text{mm}$ ( $c_{flow} = 192\text{m/s}$ )	Max. resolution of frequency ( $f_{min} = c_{flow}/d_{probe}$ )	$f_{min} = 160\text{ kHz}$ ( $c_{flow} = 192\text{m/s}$ )
Stability of the machine at the operating point (BP)	$678 \pm 1$ measuring point per revolution	Minimum resolution of the frequency determined from spectra density	$f_{min} = 100\text{Hz}$

Table 2 Characteristic data of the measurement campaign at BP with reference to the measurement objectives and the characteristic data of the compressor

The following considerations are included in Table 2. The measurement grid is determined by the number of traverse points (13) in the z direction and by m, the number of samples between the passage of two blades, which is defined by the rotational speed of the machine, number of blades and the sampling frequency as  $m = f_s / (n \cdot N)$ . The averaged magnitude of the dynamic head of 200mbar leads to signal to noise ratio of 70dB. This means that the full dynamics of the measurement electronics had to be used. The measuring time span influences the accuracy a of the ensemble averaged pressure values

$p_1(t)$ ,  $p_2(t)$ ,  $p_3(t)$  by way of equation (1), where  $a$  is the confidential interval. The confidential interval  $a$  indicates the statistical certainty of the ensemble averaged pressure values  $\bar{p}$ .

$$a = \frac{\sigma \cdot C(P, m)}{\sqrt{m}} = \frac{63.3\text{mbar} \cdot 1.96}{\sqrt{242}} = 7.9\text{mbar} \quad (1)$$

### Data conversion, analysis and interpretation

The sensor voltages are converted into pressure and temperature signals by model based reconstruction using the sensor and aerodynamic calibration data.

A dedicated software package has been developed for the comprehensive task of data processing. This performs the data conversion for an entire traverse and prints the results in a variety of menu-selected diagrams. The program is based on the „AW-System“ developed as an interactive environment for the evaluation of large time series (HERTER et al. 1992).

With the present objectives of the measurement campaign and the measurement concepts chosen, data analysis obtains a high importance for the optimization of the overall data processing. Data analysis involves several topics such as averaging methods, time-resolved spectra, autocorrelations, statistic tools for the investigation of turbulence and data filtering. The use of averaging methods applied for time-resolved and fluctuating data is discussed in this paper.

### ENSEMBLE-AVERAGED PROCEDURES FOR COMPRESSING TIME DEPENDENT INFORMATION

For the present measurements, a 1-sensor probe was operated in the pseudo 3-sensor mode. To link the three non-synchronous pressure measurements  $p_1(t)$ ,  $p_2(t)$ ,  $p_3(t)$ , made under constant operating conditions, ensemble averaging has to be utilized. (In non-modulated flow, e.g. pipes or nozzles, simple time averaging would suffice.) In modulated flow ensemble averaging has to be based on the time period of the phenomenon to be studied, e.g. the shaft revolution period, or the period of mild surge or rotating stall. In the first case triggering can be done by a geometric signal; in the second case, a flow-dependent signal must be used.

**Rotor-based ensemble averaging methods.** The *revolution ensemble averaging* method requires a sharp trigger signal sent at each revolution of the rotor. At one of these signals the time index  $n$  is set to zero, and measurement begins. After  $m$  shaft revolutions, measurement is stopped.

$$\bar{x}(t_n, z) = \frac{1}{m} \sum_{i=1}^m x_i(t_n, z) \quad (2)$$

Equation (2) quantifies the deterministic rotor-based fluctuation of the pressures  $\bar{p}_1(t)$ ,  $\bar{p}_2(t)$ ,  $\bar{p}_3(t)$ . In case of *blade to blade* or *twin-blade ensemble averaging* Eq. (2) holds, but  $n$  and  $m$  refer to the trigger signal given after each blade or twin blade passing

Stochastic fluctuations only appear statistically. They are characterized by the ensemble standard deviation, defined by

$$\bar{\sigma}(t_n, z) = \sqrt{\frac{1}{m} \sum_{i=1}^m (x_i(t_n, z) - \bar{x}(t_n, z))^2} \quad (3)$$

In case of measurements made at the outlet of the impeller and at BP running conditions (no surge etc.) the stochastic part of the pressure

fluctuations contains the information about the turbulence intensity.

**Flow-based ensemble averaging methods.** These are used for the investigation of periodic flow instabilities like mild surge. In this case the trigger signal is independent of rotor revolutions and is gained from an event related flow condition. Such trigger signals usually have variable period length and the number of measured data between two trigger events is not constant. A period related „class averaging“ method has to be used, as described in Part 2. The number of classes determines the resolution in time and the statistical accuracy of the averaging process. The number of classes, 2500 in this measurement campaign for MS, corresponds to a time step of 0.002ms (frequency=45kHz) and gives 180-200 data points per class to be averaged.

In case of MS, the trigger period is totally unrelated to the rotor revolution. This means that pressure fluctuations caused by blade passing appear as noise. In the stochastic part of the pressure fluctuations, turbulence and the periodic blade passing are both present, giving a high level of standard deviation.

### Comparison of the ensemble averaging methods

The revolution ensemble averaged pressure  $\bar{p}_1(t)$  gained from the 1-sensor-probe determined from preliminary information on the local time averaged flow direction is presented in Fig. 4.

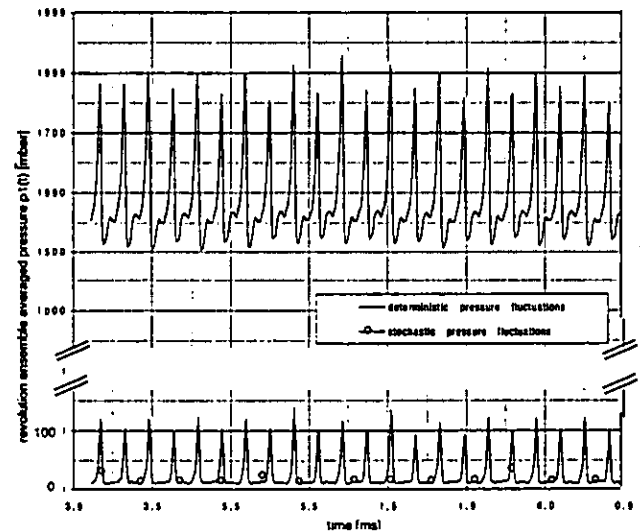


Fig. 4 Revolution ensemble averaged pressure  $\bar{p}_1(t)$  during one impeller revolution (deterministic part of the pressure fluctuation) and the stochastic part represented through the ensemble standard deviation. Running conditions: BP; outlet of impeller, traverse position  $z/b=0.18$ .

The probe was set at a traverse position  $z/b=0.18$ . The wakes of the blade trailing edges of the 11 splitter and 11 full blades are visible as peaks. The total pressure rises in the blade wakes from 1510mbar to 1780mbar which is equal to a fluctuation level in the deterministic part of the total pressure of 20% from the mean value. In the blade wakes the ensemble standard deviation (stochastic part) in Fig. 4 rises from a low level of 10mbar to a maximum of 137mbar. This corresponds to 8% of the mean pressure level of  $\bar{p}_1(z)=1587\text{mbar}$ . The deterministic and stochastic fluctuations of the pressure  $p_1(t)$  are a quantity to characterize

the flow in a compressor. There has to be a dissipation process to level out these fluctuations.

In Fig. 5 the standard deviation of the deterministic and stochastic parts of the ensemble averaged  $p_1(t)$  pressure fluctuations are plotted across the channel width, as measured at position 1 under BP conditions. The curves A represent the standard deviation of the *deterministic* fluctuation around the time-mean pressure  $\bar{p}_1$ . The curves B represent the standard deviation of the *stochastic* fluctuations around the instantaneous deterministic value. It is seen that the deterministic  $p_1$  fluctuations dominate at position 1 over the stochastic events; i.e., the blade wakes are the dominant unsteady effect. Furthermore, both parts of the pressure fluctuation decrease toward the shroud where the flow velocity is very low (see  $c_r$  in Fig. 6) and where the wakes are such that the velocity direction (in yaw) fluctuates much less than near the hub. (Yaw fluctuation data are not shown for lack of space.)

During each revolution of the shaft, a sequence of 11 main blades and 11 splitter blades passes the probe. Ensemble averaging can be based on different periods. If the flow period of interest is a complete revolution of the shaft, the time series  $p_1(t)$  is compressed to the time duration  $\Delta t_R = 1/N$ . Another period of interest is  $\Delta t_T = 1/11N$ , i.e. the passage time of a blade twin. Both types of ensemble averaging have been tested. The revolution ensemble averaging gave curves A1 and B1, while twin-blade averaging gave A2 and B2. It is seen that both methods yield closely identical fluctuations, indicating that all blade pairs of the impeller have closely identical geometry and therefore, there are no low-order ( $<11$ ) harmonics of  $N$  present in the flow.

A further period is  $\Delta t_T = 1/22N$ ; i.e. the passage time of a blade to blade section. The deterministic fluctuations are shown separately for the channel between the splitter blade and the pressure side of the full blade versus the channel between the suction side of the full blade and the splitter blade. These ensemble averaging gave curve A3 and A4. The difference between these curves indicates that the flow leaving every second impeller channel is different, see Part 2. The stochastic fluctuations have approximately the same magnitude as curve B1 and B2.

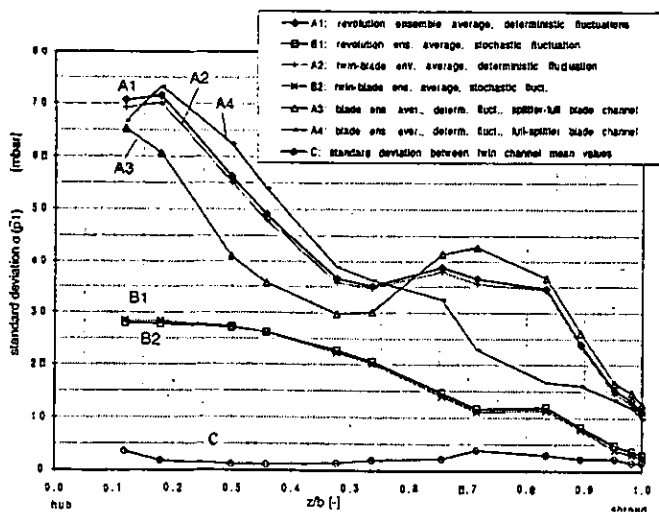


Fig. 5 Averaged deterministic and stochastic pressure fluctuation over traverse position ( $z/b$ ) obtained from different ensemble averaging strategies. Running conditions: BP; impeller outlet, position 1.

Line C in Fig. 5 shows the standard deviation of the 11 mean values  $\bar{p}_1(t)$  obtained for each of the 11 blade channel twins. This variation is a measure for the existence of a „finger print“ of the impeller. All impeller blade pairs have closely identical geometry and there are no low frequencies in the signal which arise from the interaction of the impeller with the diffuser blades.

In Fig. 6 the time averaged radial velocity  $c_r$  (black diamond symbols) and the standard deviation of the deterministic  $c_r$  fluctuations (triangle) are presented. The  $c_r$  fluctuations are moderate. They are strongest in mid-channel and decline toward the shroud (where  $c_r$  is low anyway) and toward the hub where  $c_r$  is high but fluctuates little. The tangential velocity fluctuations are of similar magnitude (circle symbols). It is important to note that these modest values of the velocity standard deviations do not mean that high instantaneous peaks or dips do not occur. In fact wake-induced deterministic peaks may exceed the standard deviation level by a factor of three or more (GIZZI et al., 1999).

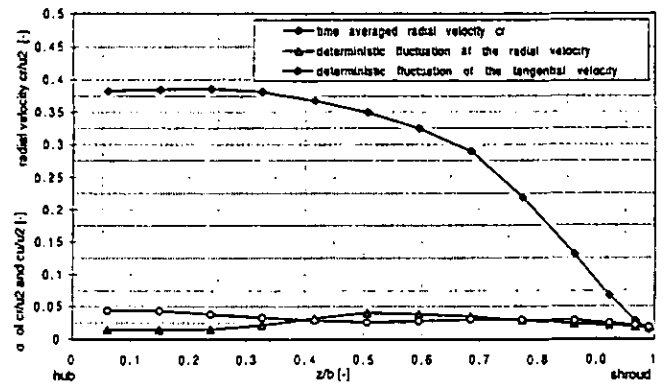


Fig. 6 Time-mean velocity profile and averaged deterministic radial fluctuations over traverse position ( $z/b$ ). Running conditions: BP.

Averaging methods have to deal with either or both kinds of nonuniformities, namely the spatial (hub to tip) distribution and the temporal (i.e., circumferential) fluctuations.

## COMPARISON OF AVERAGING METHODS

### Coordinates

Fig. 7 shows the cylindrical coordinates used. Note that the circumferential angle  $\theta$  is related to measurement time  $t$  as

$$d\theta = 2 \cdot \pi \cdot N \cdot dt \quad (4)$$

and the flow area is given by

$$dA = r_E \cdot d\theta \cdot dz = u_E \cdot dt \cdot dz \quad (5)$$

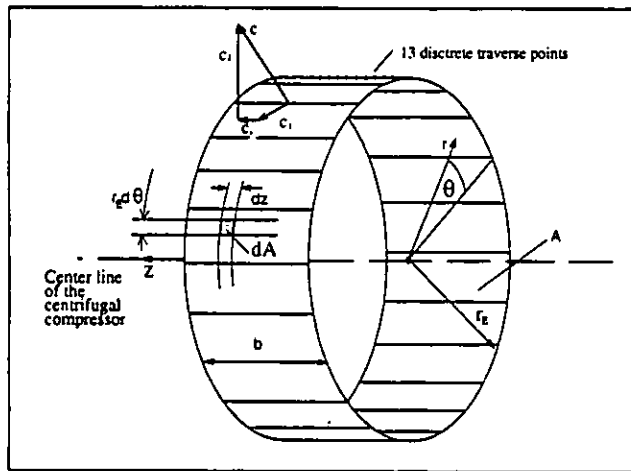


Fig. 7 Coordinate system used.

### Averaging

Averaging can be done circumferentially only (*time averaging*, see Eq. (6)), axially only (*spanwise averaging*, see Eq. (7)) or over the surface area  $dA$  (*annular averaging*, see Eq. (8)).

- Time averaging yields spanwise distributions over the channel width  $b$

$$\frac{1}{t_0} \cdot \int x(t, z) dt \equiv \bar{x}(z) \quad (6)$$

- Spanwise averaging gives time functions

$$\frac{1}{b} \cdot \int x(t, z) dz \equiv \bar{x}(t) \quad (7)$$

- Annular averaging yields constant numbers

$$\frac{1}{b \cdot t_0} \cdot \int x(t, z) dt dz \equiv \bar{x} \quad (8)$$

In the following, averaging theories are formulated for annular averaging. The equations obtained can be easily modified for the timewise or spanwise averaging presented above.

Here  $X(t, z)$  may represent any type of flow-dependent quantity or group. Physically meaningful concepts for defining functions  $X$  have been established by TRAUPEL (1988) and DZUNG (1967). The aim of these concepts is to provide average values that are relevant from the point of view of turbomachinery theory; i.e. strictly respect the conservation laws of mass, momentum and energy and therefore fulfill the mass, force and energy balances. Following flow quantities are measured by a „pseudo 3-sensor probe“:

velocity:	$c_r(t, z);$	$c_t(t, z)$
pressure:	$p_{stat}(t, z);$	$p_{stat}(t, z)$
temperature:	$T_{rec}(z);$	

Due to the thermal inertia of the probe, temperature is not resolved over time, unfortunately.

The probe measures a recovery temperature lying between the time- mean static and total temperature values. With the recovery factor being known from calibration ( $r \approx 0.7$ , see Part 1), the time-mean static and total flow temperatures are obtained as

$$T_{stat}(z) = T_{rec}(z) - \frac{r}{2c_p} \cdot \overline{c(t, z)^2} \quad (9)$$

$$T_{tar}(z) = T_{rec}(z) + \frac{1-r}{2c_p} \cdot \overline{c(t, z)^2} \quad (10)$$

The average of  $c^2$  will be defined below.

The gas equation of state yields local density  $\rho$  and enthalpy  $h$  as

$$\rho = p / (RT_{stat}) \quad (11)$$

$$h = c_p(T_{stat}) \cdot T_{stat} \quad (12)$$

The velocity components  $c_r$  and  $c_t$  are equivalent to specifying angle  $\varphi$  and magnitude  $c$ . (Note that 2D planar flow is treated here. A third component ( $c_z$ ) would require the use of four or five sensor probes.)

### Averaging method according to Traupel

The convectively transported flux of a mass-specific flow quantity  $x$  through area  $dA$  (Fig. 7) in unit time is given by  $x\rho c_r dA$ . The mass flow rate through an annulus surface  $A$  is given by

$$\dot{m} = \int_A p(t, z) \cdot c_r(t, z) dA \quad (13)$$

The annulus average of  $x$  per unit mass is therefore

$$\bar{x} = \frac{1}{\dot{m}} \cdot \left( \int_A x(t, z) \cdot \rho(t, z) \cdot c_r(t, z) \right) dA \quad (14)$$

The procedure to average annulus flow data with Traupel's method is to determine an annulus-average radial velocity  $\bar{c}_r$  from Eq. (14) by setting  $x=c_r$ , which amounts to averaging the radial momentum flux. Next, a mean tangential momentum flux  $\bar{r}c_t$  is determined from Eq. (14) by setting  $x=r(z)c_t(t, z)$ . The annulus average static enthalpy  $\bar{h}$  is obtained by setting  $x=h(t, z)=c_p T_{stat}(z)$ , and the ann. averaged total enthalpy results as

$$\bar{h}_{tar} = \bar{h} + \overline{c^2} / 2 \quad (15)$$

(Some error is introduced by the lack of time-resolved temperature data in the present experiments.) The mean kinetic energy flux  $\overline{c^2} / 2$  is obtained by setting  $x = [c_r^2(t, z) + c_t^2(t, z)] / 2$ .

For averaging the static pressure Traupel recommends a simple (unweighted) area averaging in order to conserve pressure forces in momentum balances. He defines the annulus average pressure as

$$\bar{p} = \frac{1}{A} \cdot \int p(t, z) dA \quad (16)$$

With  $\bar{p}$  and  $\bar{h}$  known, the gas equations are used to calculate a mean density  $\bar{\rho}$  as

$$\bar{\rho} = \rho(\bar{p}, \bar{h}) = (c_p / R) \cdot \bar{p} / \bar{h} \quad (17)$$

The above momentum-based definition of  $\bar{c}_r$  does not satisfy the continuity equation in its simplest form,

$$\dot{m} \neq \bar{\rho} \cdot \bar{c}_r \cdot A \quad (18)$$

because Eq. (13) requires a kind of averaging different from Eq. (14).

The correctness of mass flow is restored by Traupel by defining a „continuity shape factor“  $\epsilon_k$  for the radial velocity profile as

$$\dot{m} = \bar{p} \cdot (1 - \epsilon_k) \cdot \bar{c}_r \cdot A \quad (19)$$

$$1 - \epsilon_k = \int_A \frac{\rho(t, z)}{\bar{p}} \cdot \frac{c_r(t, z)}{\bar{c}_r} \cdot \frac{dA}{A} \quad (20)$$

Further, the mean tangential momentum flux  $\bar{r}c_t$  does not automatically define a mean tangential velocity component  $\bar{c}_t$ . For defining  $\bar{c}_t$  some reference radius  $\bar{r}^*$  has to be specified, as e.g.

$$\bar{c}_t = \bar{r}c_t / \bar{r}^* \quad (21)$$

Dzung has called  $\bar{r}^*$  the „Euler radius“ and conveniently defined it as the radius at which the mean absolute-frame and rotor-frame velocities  $c_t$  and  $w_t$  are vectorially additive according to  $c_t = \omega\bar{r}^* + w_t$ . He found that  $\bar{r}^*$  is obtained as

$$\bar{r}^* = \left[ \frac{1}{\dot{m}} \cdot \int_A \rho c_r r^2 dA \right]^{1/2} \quad (22)$$

In case of a cylindrical surface, as in the present case,  $\bar{r}^*$  equals the cylinder radius.

The specific kinetic energy of the fluid is represented by

$$\frac{\bar{c}^2}{2} = \frac{(\bar{c}_r)^2 + (\bar{c}_t)^2}{2} \quad (23)$$

However, as in the case of mass flux, the kinetic energy flux also requires a correction, because  $\bar{c}^2/2$  is not identical to  $(\bar{c}^2)/2$  defined above. Traupel introduces an „energy shape factor“  $\epsilon_e$  to the velocity  $\bar{c}$  obtained from momentum averaging as

$$(\bar{c}^2) = [(1 - \epsilon_e) \cdot \bar{c}]^2 \quad (24)$$

yielding the relation

$$\bar{h}_{tot} = \bar{h} + [(1 - \epsilon_e) \cdot \bar{c}]^2 / 2 \quad (25)$$

In summary, Traupel defines all velocity components by momentum averaging, but needs various shape factors to conserve mass and energy. In case of uniform flow, these become  $\epsilon_k = \epsilon_e = 0$ .

### Averaging method according to Dzung

Dzung's „consistently“ averaged values are defined to comply with mass, momentum and energy conservation and avoid shape factors as described in DZUNG (1967). For this purpose kinetic energy is defined as

$$\frac{\bar{c}_{Dz}^2}{2} = \frac{\bar{c}_{rDz}^2}{2} + \frac{\bar{c}_t^2}{2} \quad (26)$$

where  $\bar{c}_t$  follows from Eq. (21) and  $\bar{c}_{rDz}$  is the continuum average of the radial component obtained with Eq. (14) from

$$\dot{m} = \bar{p}_{Dz} \cdot \bar{c}_{rDz} \cdot A = \int_A \rho(t, z) \cdot c_r(t, z) dA \quad (27)$$

In order to conserve total enthalpy in adiabatic flow according to the First Law

$$\bar{h}_{tot} = \bar{h}_{Dz} + \frac{\bar{c}_{Dz}^2}{2} \quad (28)$$

Dzung adapts the definition of static enthalpy as

$$\bar{h}_{Dz} = \frac{1}{\dot{m}} \cdot \int_A h_{tot}(t, z) \cdot c_r(t, z) \cdot \rho(t, z) dA - \left( \frac{\bar{c}_{rDz}^2}{2} + \frac{\bar{c}_t^2}{2} \right) \quad (29)$$

Compliance with momentum conservation is achieved by adapting the definition of static pressure as

$$\bar{p}_{Dz} = \bar{p} + \frac{1}{A} \cdot \int \rho(t, z) c_r^2(t, z) dA - \frac{\dot{m} \cdot \bar{c}_{rDz}}{A} \quad (30)$$

where  $\bar{p}$  is the area averaged pressure determined with Eq. (16). With the static pressure  $\bar{p}_{Dz}$  and the enthalpy  $\bar{h}_{Dz}$  the density  $\bar{\rho}_{Dz}$  can be determined by the gas equations as

$$\bar{\rho}_{Dz} = \rho(\bar{p}_{Dz}, \bar{h}_{Dz}) \quad (31)$$

With the density  $\bar{\rho}_{Dz}$  known, the radial velocity  $\bar{c}_{rDz}$  can iteratively be calculated again by Eq. (27).

Dzung averaging is formally simple, but flow incidence angles calculated from  $\bar{c}_{rDz}$  and  $\bar{c}_t$  may be misleading in flows with strongly non-uniform velocity profiles.

### Simple arithmetic time averaging

Finally, in order to compare the above averaging methods with simple (i.e., non-physical) arithmetic timewise and spanwise averaging, we also calculate

$$\bar{x} = \frac{1}{\Delta z \Delta t} \cdot \iint x(t, z) (dt)(dz) \quad (32)$$

### Comparison of the averaging methods

For the comparison of the three averaging methods in the highly fluctuating centrifugal compressor impeller outlet flow field, the stage work is calculated first by inserting the averaged velocity components  $c_t$  obtained above into the Euler momentum equation. Due to the straight axial flow at the impeller inlet,  $c_{t1}$  is zero and the stage work is

$$\bar{a}_a = \bar{u}_E \cdot \bar{c}_{tE} \quad (33)$$

The differences between the various methods must be viewed in terms of measuring accuracy. The measurement errors of the velocities  $c_{tE}$  are about 0.5% of the velocity mean value for velocity levels above 50m/s, 1% for levels under 50m/s. The accuracy of the differential pressure measurement  $\Delta p_E$  is defined with the standard deviation of the residuals having a magnitude of 0.2mbar for a dynamic head of 250mbar. The measurement accuracy for the absolute pressure is 0.1‰ corresponding to 0.17mbar for a pressure value of about 1700mbar (see, Part1). Dynamic errors of a cylindrical probe are described in HUMM et al. (1995) and a comparison between FRAP<sup>®</sup> and LDA measurements in the present centrifugal compressor is presented in GIZZI et. al. (1999).

#### a) Circumferential (timewise) averaging: $\int x(t, z) dt$

The stage work distribution across the diffuser channel (z/b) calculated from Eq. (33), with the circumferential velocity mean gained with different averaging methods is shown in Fig. 8. The three curves virtually coincide.



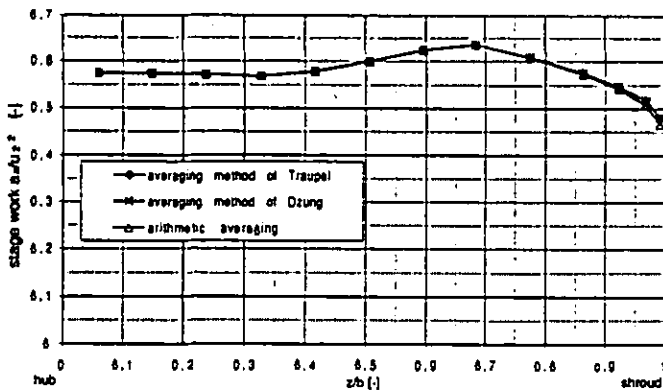


Fig. 8 Stage work  $a_a$  across the traverse obtained from different averaging methods. Running conditions: BP.

Due to the shape factor  $\epsilon_k$  defined in the averaging method of Traupel as a mass flow correction, the tangential velocity component  $c_t$  calculated with the method of Traupel is identical with the  $c_t$  obtained with Dzung. According to Eq. (29) both averaging methods lead to equal stage work values. The difference between the arithmetically time-averaged stage work and the values gained with the thermodynamic averaging methods increases from 0.2% at the hub to 2.5% at the shroud. The mean difference over the span is a mere 0.4% of the work. This is close to the measurement accuracy itself; i.e., negligible.

The radial velocity  $c_r$ , calculated with the three averaging methods is shown in Fig. 9. The mean differences between the averaging method of Traupel and Dzung across the traverse is 2%.

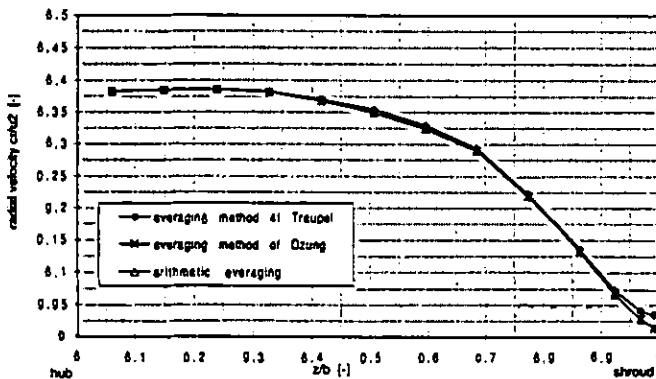


Fig. 9 Radial velocity across the traverse obtained from different averaging methods. Running conditions: BP.

In the averaging model of Traupel, the shape factor  $\epsilon_k$  defined by Eq. (20) considers boundary layers and provides an effective area  $A$ . Due to the smaller area  $A$ , the velocity component  $c_r$  has a higher magnitude for the model of Traupel.  $\epsilon_k$  is dependent on the fluctuation intensity of  $c_r$ .

The static pressure is presented in Fig. 10 and calculated with three averaging methods.

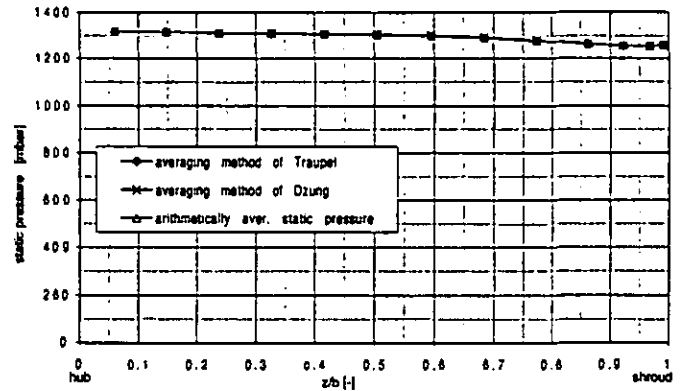


Fig. 10 Static pressure across the traverse obtained from different averaging methods. Running conditions: BP.

The difference between the static pressure calculated with the averaging method of Dzung and the area averaged pressure from the method of Traupel is less than 0.05% across the traverse at position I. This equals 0.3% of the mean dynamic head. The measurement error for the pressure is lower than the differences between the averaging methods.

#### b) Spanwise averaging: $\int x(t, z) dz$

For the comparison of axially averaged flow quantities based on the three methods, data measured during MS running conditions are used, because the time evolution of such hub-to-shroud averages is mainly of interest during unsteady operating conditions. The averaged data have to be class averaged to get the time dependent flow quantities  $c_r(t, z)$ ,  $c_t(t, z)$ ,  $p_{stat}(t, z)$ , see Part 2.

Figure 11 shows the spanwise averaged momentary stage work during one MS cycle, as calculated with three averaging methods. There is a net difference between the physical averaging methods (Traupel and Dzung) and the physically blind arithmetic average. The mean difference during one „mild surge“ period is about 1.26kJ/kg, or 2.7%.

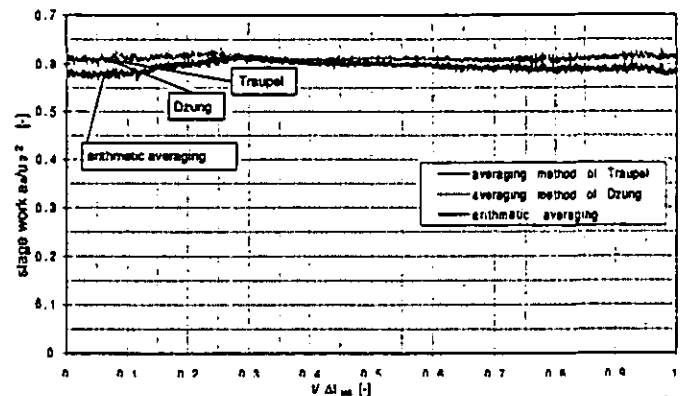


Fig. 11 Stage work during a MS period obtained from different averaging methods. Running conditions: MS.

The fluctuation of radial velocity  $c_r$  during a MS period is presented in Fig. 12. Due to the high axial non-uniformity of the measured radial

velocity  $c_r$ , the differences between the averaging methods of Traupel and Dzung amount to 16% during the whole period. This illustrates the difference between momentum-based (Traupel) and continuity based (Dzung or Traupel  $(1 - \epsilon_k)c_r$ ) averages.

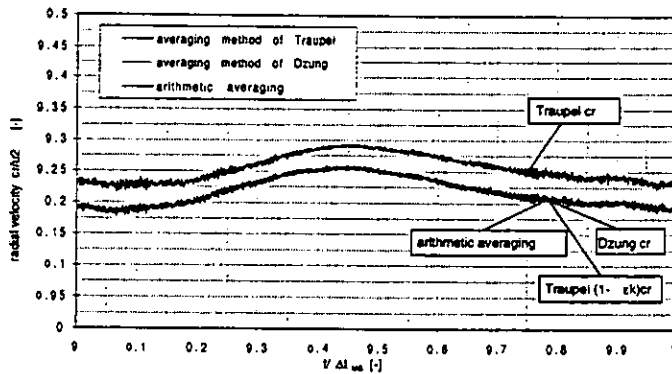


Fig. 12 Radial velocity during a MS period obtained with different averaging methods. Running conditions: MS.

All averages in Fig. 11 and Fig. 12 are seen to fluctuate during an MS cycle, the mass flow ( $c_r$ ) having a much higher amplitude than the stage work. The near constancy of work can be shown to be due to the constancy of the tangential ( $c_t$ ) component in the hub half of the channel where most work transfer occurs<sup>1</sup>. In the coexistence of high mass flow amplitudes with low work (or pressure head) amplitudes is not surprising in an operating point where the head vs. flow characteristic of the stage is almost horizontal (see Fig. 7 in Part 2).

The static pressure differences between the averaging methods of Traupel and Dzung (not shown here) depend on the velocity fluctuation and have a value of 0.5% over the entire MS period, while the static pressure amplitude was of the order of 10%

c) Annular averaging:  $\int x(t, z) dt dz$

$\int x(t, z) dt dz$	averaging method of Traupel	averaging method of Dzung	arithmetic averaging
stage work	43.68kJ/kg	43.68kJ/kg	42.43kJ/kg
velocity $c_r$	0.345 $c_r/u_2$ [-]	0.30 $c_r/u_2$ [-]	0.25 $c_r/u_2$ [-]
velocity $c_u$	0.59 $c_u/u_2$ [-]	0.59 $c_u/u_2$ [-]	0.57 $c_u/u_2$ [-]
static pressure	1296mbar	1297mbar	1290mbar

Table 3 Annulus averaged flow quantities determined with three averaging methods. Running conditions: BP.

- The arithmetically averaged work is lower than the physical averages because the flow-deficient shroud-side region, where the work transfer is poor, are more heavily weighted.

For the comparison of the averaging methods in both scanning directions ( $t$  and  $z$ ) the circumferential ensemble averaged data for the operation point BP at probe position I have been calculated

In Table 3 the velocity components, the static pressure and the stage work calculated with the averaging methods of Traupel and Dzung and as simple arithmetic averages are presented for BP running conditions at position I. The flow quantities are first timewise averaged and then spanwise. The standard deviation of the  $c_r$  distribution gets a high level after the first timewise averaging of 56% for the method of Dzung and 55% for the method of Traupel. This highly inhomogeneous flow across the traverse leads to differences between the averaging methods, especially with respect to the radial velocity component. The differences between the two physically founded methods stem from using different definitions for  $\bar{c}_r$ .

### SUMMARY AND CONCLUSIONS

- The comparisons presented in this paper were made for two running conditions of a centrifugal compressor, „best point“ and „mild surge“, with the rig operated in the stable and the unstable branch of the operating line, respectively.
- The data processing of time-resolved FRAP<sup>®</sup> signals comprises data conversion, data analysis and interpretation using measurement concepts adapted to the individual goals of the measurement campaign.
- The revolution-based and blade-twin-based ensemble averaging methods are discussed. Deterministic pressure fluctuations near the hub reach 35% of the averaged dynamic head and 5% near the shroud. The differences between the two ensemble averaging methods are negligible across the diffuser channel. The stochastic fluctuations are much lower than the deterministic ones.
- The averaging methods of Traupel, Dzung and arithmetic averaging are applied to the time-resolved data. Three averages, namely axial, circumferential, and channel surface, are presented.
- Even though the circumferential fluctuations of velocity and pressure in the impeller outlet flow are significant, the circumferential averaging methods yield closely identical axial distributions. However, the spanwise averaged values differ considerably due to the very low radial through flow existing near the shroud.

### REFERENCES

Adamczyk.J.J., 1985. „A Model for Closing the Inviscid Form of the Average-Passage Equation System“, *ASME Paper 86-GT-227*

Casartelli, E., Saxer, A. P., and Gyarmathy, G., 1997. „Numerical Flow Analysis in a Subsonic Vaned Radial Diffuser with Leading Edge Redesign“, *ASME Paper 97-GT-185*

Dean, R.C.Jr., Senoo, Y., 1960, „Rotating Wakes in Vaneless Diffusers“, *Journal of Basic Engineering, Sept 1960.*

Dzung L.S., 1967, „Mittelungsverfahren in der Theorie der Schaufelgitter“, *Brown Boveri Mitteilungen, January 1967.*

Dzung L.S., 1970, „Flow Research on Blading“, *Proceedings of the Symposium on Flow Research on Blading, 1969.*

Eckardt, D., 1975, „Instantaneous Measurements in the Jet-Wake Discharge Flow of a Centrifugal Compressor Impeller“, *Journal of*

Downloaded from http://asmedigitalcollection.asme.org/GT/proceedings-pdf/GT1999/788583/V001T03A033/4215674/400103a033-99-gt-154.pdf by ETH Zuerich user on 20 August 2020

*Engineering for Power*, July 1975.

Gerhard, P.M., 1981, „Averaging Methods for Determining the Performance of Large Fans from Field Measurements“, *Journal of Engineering for Power*, April 1981.

Gizzi, W., Roduner, C., Stahlecker, D., Köppel, P., Gyarmathy, G., „Time Resolved Measurements with Fast-Response Probes and Laser-Doppler-Velocimetry at the Impeller Exit of a Centrifugal Compressor - A Comparison of Two Measurement Techniques“, to be publ. in 1999, *3rd European Conference on turbomachinery*.

Gossweiler, C., Humm, H. J., and Kupferschmied, P., 1992, „Development of a System for Aerodynamic Fast-Response Probe Measurements“, *Proc. of the 18th Congress of Int. Council of the Aeronautic Sciences (ICAS)*, Beijing.

Gossweiler, C., Kupferschmied, P., and Gyarmathy, G., 1995, „Dn Fast-Response Probes. Part 1: Technology, Calibration and Application to Turbomachinery“, *Journal of Turbomachinery*, Vol. 117/4.

Herter, D., Chrisander, O., and Gossweiler, C., 1992, „AW-System - An Interactive Environment for the Evaluation of Large Time Series“, *Proc. of the 11th Symposium on Measuring Techniques for Transonic Flows in Cascades and Turbomachines*, Munich, Germany

Humm, H. J., Gossweiler, C., and Gyarmathy, G., 1995, „On Fast-Response Probes. Part 2: Aerodynamic Design Studies“, *Journal of Turbomachinery*, Vol. 117/4.

Hunziker, R., 1993, „Einfluss der Diffusorgeometrie auf die Instabilitätsgrenze des Radialverdichters“, *PhD-thesis No. 10252*, ETH Zürich, Switzerland

Kupferschmied, P., Gossweiler, C., and Gyarmathy, G., 1994, „Aerodynamic Fast-Response Probe Measurement Systems: State of Development, Limitation and Future Trends“, *Proc. of the 12th Symposium on Measuring Techniques for Transonic and Supersonic Flows in Cascades and Turbomachines*, Prague, Czech Republic.

Kupferschmied, P., 1998, „Zur Methodik zeitaufgelöster Strömungs sondennmessungen in Verdichtern und Turbinen“ *PhD-thesis No. 12774*, ETH Zürich, Switzerland.

Kreitmeier, F. Juvet, P.J., 1997, „Demonstration of a Balance-Based Procedure for Time-Averaging and Modeling of Compressible Three-Dimensional Unsteady Turbulent Flows“.

Ng, W. F., and Epstein, A. H., 1985, „Unsteady Losses in Transonic Compressors“, *Journal of Engineering for Gas Turbines and Power*, Vol. 107 / 345-353

Roduner, C., Köppel, P., Kupferschmied, P., Gyarmathy, G., 1998, „Comparison of Measurement Data at the Impeller Exit of a Centrifugal Compressor Measured with both Pneumatic and Fast-Response Probes“, *ASME Turbo Expo '98*, 98-GT-241, Stockholm

Ruck, G., 1989, „Verfahren zur instationären Geschwindigkeits- und Turbulenzmessung mit einer pneumatisch messenden Keilsonde“, *Mitteilungen des Institutes Nr. 33*, Institut für Thermische Strömungsmaschinen und Maschinenlaboratorium der Universität Stuttgart, Stuttgart, Germany.

Stahlecker, D., and Gyarmathy, G., 1998, „Investigations of Turbulent Flow in a Centrifugal Compressor Vaned Diffuser by 3-Component Laser Velocimetry“, *ASME Turbo Expo '98*, Stockholm, Sweden.

Traupel, W., 1988, „Thermische Turbomaschinen I“, Springer-Verlag, Berlin, p. 307